ЖЭТФ, 2014, том 145, вып. 5, стр. 816–824

SPONTANEOUS DECAY RATES OF THE HYPERFINE STRUCTURE ATOMIC STATES INTO AN OPTICAL NANOFIBER

A. V. Masalov [a]*, ***V. G. Minogin*** [b]**

[a] *Lebedev Physical Institute, Russian Academy of Sciences*
119991, Moscow, Russia

[b] *Institute of Spectroscopy, Russian Academy of Sciences*
142190, Troitsk, Moscow, Russia

Received November 20, 2013

Spontaneous decay rates of atoms into guided modes of an optical nanofiber are found for atomic transitions between the hyperfine structure sublevels. The decay rates are evaluated for the hyperfine structure transitions in Rb atoms. The efficiency of the guided mode excitation by spontaneous decay of the specific hyperfine atomic states is examined for both the fundamental fiber mode HE_{11} and the higher-order modes TE_{01}, TM_{01}, and HE_{21}.

DOI: 10.7868/S0044451014050048

1. INTRODUCTION

Recently, there has been an increasing interest in the interactions between optically excited atoms and dielectric nanobodies, such as optical nanofibers, nanospheres, and nanodisks. This is mostly due to the potential such systems offer for controlling and manipulating single atoms, and also due to the potential of the systems as regards controlling light propagation inside optical nanostructures. From a more general standpoint, optical nanostructures can be regarded as interfaces that allow connecting the atoms located near nanostructures with the electromagnetic fields propagating inside the nanostructures and accordingly control the states of both the atoms and photons guided inside the nanostructures. Known examples of such interface phenomena are the enhanced spontaneous emission of optically excited atoms into the nanofiber fundamental guided mode [1–4], the red shift of light spontaneously emitted by atoms located near nanofibers or nanospheres [5–10], and excitation of atoms trapped around optical nanofibers by light propagating along the nanofibers [11–14]. New interface phenomena may arise in experiments devoted to entanglement between distant trapped atoms via the guided modes of the nanofiber [15, 16]. In particular, efficient excitation of the higher-order guided modes can be achieved by spontaneous emission of atoms located near the nanofiber interfaces [17].

One of the most efficient techniques that allow coupling the atoms and the electromagnetic field of a nanofiber is the pumping of the guided modes of a nanofiber by spontaneous emission of optically excited atoms. This technique has been experimentally verified for Cs atoms and proved to have very high efficiency [6]. In the research on pumping the guided modes of optical nanofibers by spontaneous emission of atoms, a two-level atomic scheme has so far been considered as a basic model. The only extension of this model was given in paper [15], which considered the transition between atomic states degenerate over magnetic sublevels with the example of a Cs atom. The present-day experiments basically use the atoms, such as Rb and Cs, that emit spontaneous radiation into the optical modes of nanofibers performing transitions between the hyperfine structure states. Accordingly, evaluating the spontaneous decay rates for atomic transitions between hyperfine structure states is of importance for the comparison between theoretical pumping rates and experimentally observed ones.

In this paper, we present an analysis of the spontaneous decay rates of atoms into the guided modes of optical nanofibers for a rather general scheme of hyperfine structure sublevels related to an allowed dipole

*E-mail: masalov@sci.lebedev.ru
**E-mail: minogin@isan.troitsk.ru

transition. The rates of spontaneous decays into guided nanofiber modes are given both for arbitrary hyperfine structure transitions and for the scheme relevant for ^{85}Rb atoms. The decays of an ^{85}Rb atom into the guided modes of a nanofiber are considered for both the fundamental mode HE_{11} and three higher-order modes TE_{01}, TM_{01}, and HE_{21}.

2. DECAY RATES AT TRANSITIONS BETWEEN THE HYPERFINE STRUCTURE STATES

We outline a derivation procedure for the rates of spontaneous decay of an atom into nanofiber guided modes for atomic transitions between the hyperfine structure states. We assume that the atom located near the nanofiber surface is excited by laser light and spontaneously decays, pumping the nanofiber guided modes as shown in Fig. 1. We consider spontaneous decays of the atom at the dipole transitions occuring between the hyperfine structure states $|\alpha_g F_g\rangle$ and $|\alpha_e F_e\rangle$ that are defined by the total angular momenta F_g and F_e and degenerate over the magnetic sublevels M_g and M_e as shown in Fig. 2. In such a scheme, the dipole interaction terms are to be defined with respect to the nondegenerate states $|\alpha_g F_g M_g\rangle$ and $|\alpha_e F_e M_e\rangle$.

The derivation of the spontaneous decay rates follows the Weisskopf–Wigner approach based on the

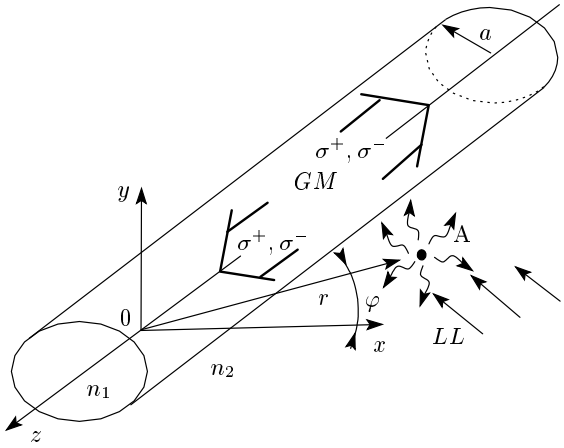

Fig. 1. Schematic of spontaneous emission of an atom into an optical nanofiber. An atom A is optically excited by near-resonant laser light LL. Spontaneous emission can excite four guided modes GM, two with the $\sigma^{\pm}$ polarization and the propagation direction $+z$, and two with the $\sigma^{\pm}$ polarization and the propagation direction $-z$

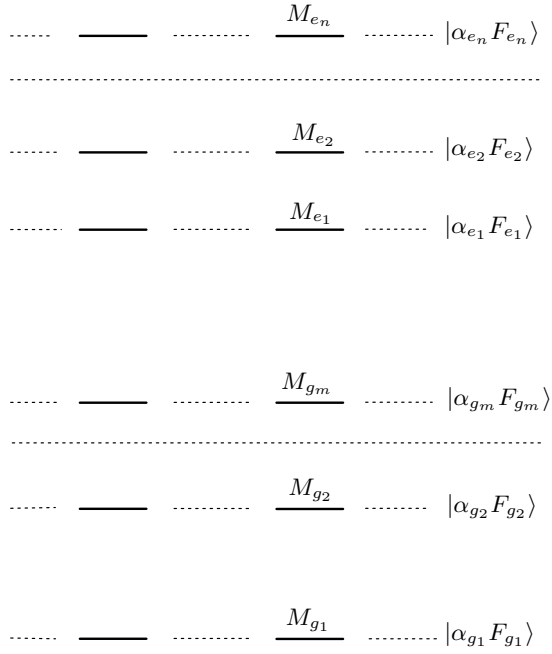

Fig. 2. The atomic level scheme describing hyperfine structure sublevels for the allowed dipole transition

Hamiltonian for a "multilevel atom+vacuum field" system taken in the rotating wave approximation:

$$H = \sum_{g,e} \hbar\omega_{eg} b_{eg}^{\dagger} b_{ge} + \sum_{\lambda} \hbar\omega_{\lambda} \left(a_{\lambda}^{\dagger} a_{\lambda} + \frac{1}{2} \right) - \\ - \sum_{\lambda,g,e} \left(\mathbf{d}_{eg} \cdot \boldsymbol{\mathcal{E}}_{\lambda} b_{eg}^{\dagger} a_{\lambda} + \mathbf{d}_{ge} \cdot \boldsymbol{\mathcal{E}}_{\lambda}^{*} b_{ge} a_{\lambda}^{\dagger} \right), \quad (1)$$

where ω_{eg} is the frequency of the atomic transition between the ground-state sublevel $|g\rangle = |\alpha_g F_g M_g\rangle$ and the excited-state sublevel $|e\rangle = |\alpha_e F_e M_e\rangle$, ω_{λ} are the photon frequencies, $a_{\lambda}^{\dagger}$ and a_{λ} are the photon creation and annihilation operators, $b_{eg}^{\dagger}$ and b_{ge} are the atomic excitation and de-excitation operators, and $\mathbf{d}_{eg}$ and $\mathbf{d}_{ge}$ are matrix elements of the atomic dipole moment. The vector $\boldsymbol{\mathcal{E}}_{\lambda}$ defines the "electric field amplitude of a single photon" with a unit polarization vector $\mathbf{e}_{\lambda}$ and the wave vector $\mathbf{k}$,

$$\boldsymbol{\mathcal{E}}_{\lambda} = i \sqrt{\frac{\hbar\omega_{\lambda}}{2\varepsilon_0 V}}\, \mathbf{e}_{\lambda} e^{i\mathbf{k}\cdot\mathbf{r}}, \quad (2)$$

where V is the quantization volume and ε_0 is the electric constant.

For Hamiltonian (1), equations for the probability amplitudes in the simplest case of a vacuum field taken initially in the vacuum state are

$$\dot{c}_{e,0} = \frac{i}{\hbar}\sum_{\lambda} \mathbf{d}_{eg}\cdot\boldsymbol{\mathcal{E}}_{\lambda}\exp(-i\Delta_{\lambda,eg}t)c_{g,1_\lambda},$$
$$\dot{c}_{g,1_\lambda} = \frac{i}{\hbar}\mathbf{d}_{ge}\cdot\boldsymbol{\mathcal{E}}^{*}_{\lambda}\exp(i\Delta_{\lambda,eg}t)c_{e,0}, \quad (3)$$

where $c_{g,1_\lambda}$ are the probability amplitudes of the states that include the ground atomic substate $|g\rangle = |\alpha_g F_g M_g\rangle$ and the vacuum field state with one photon in the mode λ, and $c_{e,0}$ is the probability amplitude of the state that includes the excited atomic substate $|e\rangle = |\alpha_e F_e M_e\rangle$ and the vacuum field state with zero photon numbers in all modes. In the above equation, $\Delta_{\lambda,eg} = \omega_\lambda - \omega_{eg}$ is the detuning of the vacuum mode frequency ω_λ with respect to the atomic transition frequency ω_{eg}.

Taking a formal solution of the second equation in the above set,

$$c_{g,1_\lambda} = \frac{i}{\hbar}\mathbf{d}_{ge}\cdot\boldsymbol{\mathcal{E}}^{*}_{\lambda}\int_{t_0}^{t}\exp(i\Delta_{\lambda,eg}t')c_{e,0}(t')\,dt', \quad (4)$$

and substituting it in the first equation, we can obtain an equation that describes the spontaneous decay of the upper atomic substate $|e\rangle = |\alpha_e F_e M_e\rangle$ to the lower substates $|g\rangle = |\alpha_g F_g M_g\rangle$:

$$\dot{c}_{e,0} = -\frac{1}{\hbar^2}\sum_{\lambda}|\mathbf{d}_{eg}\cdot\boldsymbol{\mathcal{E}}_{\lambda}|^2 \times \int_{t_0}^{t}\exp\left[i\Delta_{\lambda,eg}(t'-t)\right]c_{e,0}(t')\,dt'. \quad (5)$$

This equation is used below to determine the rates of spontaneous decays of an atom into guided modes of a nanofiber for a rather general atomic hyperfine structure scheme shown in Fig. 2.

2.1. Decay into free space

Applying Eq. (5) to the vacuum modes of free space regarded as periodic with the quantization lengths L_j,

$$k_j L_j = 2\pi n_j, \quad j = x, y, z, \quad (6)$$

and standardly summing over all possible photon states and accordingly over proper ground substates gives a well-known decay equation for the upper atomic substate $|e\rangle = |\alpha_e F_e M_e\rangle$:

$$\dot{c}_{e,0} = -\gamma_{sp}\,c_{e,0}. \quad (7)$$

Here, $\gamma_{sp} = W_{sp}(\alpha_e F_e)/2$ is half the total spontaneous decay rate from the hyperfine structure state $|\alpha_e F_e\rangle$ to all the hyperfine structure states $|\alpha_g F_g\rangle$ belonging to the ground state,

$$W_{sp}(\alpha_e F_e) = 2\gamma_{\alpha_e F_e} = 2\sum_{\alpha_g F_g}\gamma_{\alpha_e F_e,\alpha_g F_g}. \quad (8)$$

The partial spontaneous decay rate from the excited state $|\alpha_e F_e\rangle$ to the ground state $|\alpha_g F_g\rangle$ is

$$W_{sp}(\alpha_e F_e \to \alpha_g F_g) = 2\gamma_{\alpha_e F_e,\alpha_g F_g} = \frac{1}{4\pi\varepsilon_0}\frac{4}{3}\frac{|\langle\alpha_e F_e\,\|d\|\,\alpha_g F_g\rangle|^2\,\omega_{eg}^3}{(2F_e+1)\hbar c^3}, \quad (9)$$

where $\langle\alpha_e F_e\,\|d\|\,\alpha_g F_g\rangle$ is a reduced dipole matrix element for a hyperfine structure transition.

The reduced dipole matrix element $\langle\alpha_e F_e\,\|d\|\,\alpha_g F_g\rangle$ can be expressed through the reduced dipole matrix element $\langle\alpha_e\,\|d\|\,\alpha_g\rangle$ for the fine structure transition defined by the quantum numbers $\alpha \equiv nLSJI$ [18]. This gives an expression for the spontaneous decay rate between two hyperfine structure states in terms of the $6j$-symbols:

$$W_{sp}(\alpha_e F_e \to \alpha_g F_g) = 2\gamma_{\alpha_e F_e,\alpha_g F_g} = (2J_e{+}1)(2F_g{+}1)\begin{Bmatrix} J_e & F_e & I \\ F_g & J_g & 1\end{Bmatrix}^2 W_{sp}(\alpha_g \to \alpha_e),$$

$$W_{sp}(\alpha_g \to \alpha_e) = \frac{1}{4\pi\varepsilon_0}\frac{4}{3}\frac{|\langle\alpha_e\,\|d\|\,\alpha_g\rangle|^2\,\omega_{eg}^3}{(2J_e+1)\hbar c^3},$$

where $W_{sp}(\alpha_g \to \alpha_e)$ is the spontaneous decay rate at the fine structure transition $|\alpha_e\rangle \to |\alpha_g\rangle$ and J_e is the quantum number of the atomic momentum for the excited fine structure state $|\alpha_e\rangle$.

2.2. Decay into nanofiber guided modes

We represent the electric field operator of the guided modes of a nanofiber in the standard form

$$\mathbf{E} = \sum\boldsymbol{\mathcal{E}}_{\lambda}a_{\lambda} + \text{H.c.}, \quad (10)$$

where $\boldsymbol{\mathcal{E}}_{\lambda}$ is the electric field of a single vacuum guided mode and the index λ describes the direction of propagation and polarization of a single vacuum guided mode. The electric field of a single guided mode is represented similarly to Eq. (2) as

$$\boldsymbol{\mathcal{E}}_{\lambda} = i\sqrt{\frac{\hbar\omega_{\lambda}}{2\varepsilon_0 L}}\,\tilde{\boldsymbol{\mathcal{E}}}_{\lambda}\exp(i\beta_{\lambda}z + im\varphi), \quad (11)$$

where ω_λ is the mode frequency, β_λ is the propagation constant, m is the quantum number of the mode angular momentum, $\tilde{\boldsymbol{\mathcal{E}}}_{\lambda} = \tilde{\boldsymbol{\mathcal{E}}}_{\lambda}(r)$ is the normalized

amplitude of the electric field, which depends on the transverse coordinate r, and L is the length of a one-dimensional "quantization box" introduced for counting the allowed values of the propagation constant β [19].

The normalized electric field amplitude of a single guided mode is assumed to satisfy the condition

$$2\pi \int_0^\infty n^2(r) \left|\tilde{\boldsymbol{\mathcal{E}}}_\lambda\right|^2 r\, dr = 1, \tag{12}$$

where $n(r)$ is the value of the refractive index, equal to $n_1 = \sqrt{\varepsilon}$ inside the fiber and $n_2 = 1$ outside the fiber. The above representation of the vacuum field corresponds to the standard form of the vacuum field Hamiltonian represented by the second term in Eq. (1):

$$H_{vac} = 2\varepsilon_0 \varepsilon \sum_\lambda \int dV |\boldsymbol{\mathcal{E}}_\lambda|^2 \left(a_\lambda^\dagger a_\lambda + \frac{1}{2}\right) = \\ = \sum_\lambda \hbar\omega_\lambda \left(a_\lambda^\dagger a_\lambda + \frac{1}{2}\right). \tag{13}$$

For any guided mode of an optical nanofiber, the normalized electric field can be determined from Eq. (12) with the use of the eigenvalue equation for the propagation constant $\beta = \beta_\lambda$.

We now apply basic equation (5) to the vacuum guided mode of an optical nanofiber. Taking into account that the vacuum field of a single guided mode can be considered periodic in the direction of propagation with a period L,

$$\beta_n L = 2\pi n, \quad n = 1, 2, 3, \dots, \tag{14}$$

we can replace the sum over discrete numbers in Eq. (5) with an integral such that

$$\sum_\lambda \to \frac{L}{2\pi} \int d\beta.$$

After that, using the one-to-one correspondence between values of the propagation constant and frequencies of the vacuum modes, $\beta = \beta(\omega)$, and regarding β as a continuous quantity, we can replace $d\beta$ with $d\beta = \tilde{\beta}' d\omega$, where $\tilde{\beta}' = d\beta/d\omega$. This gives

$$\sum \to \frac{L}{2\pi} \int \tilde{\beta}' d\omega.$$

Next, integrating Eq. (5) over the frequency and time, we can reduce it to the decay equation

$$\dot{c}_{e,0} = -\gamma_{guid} c_{e,0}, \tag{15}$$

describing spontaneous decay of the atom between the substates $|\alpha_e F_e M_e\rangle$ and $|\alpha_g F_g M_g\rangle$ followed by excitation of the guided mode with the specific propagation direction $+z$ or $-z$ and specific circular polarization $\sigma = +1$ or $\sigma = -1$. Accordingly, the total spontaneous decay rate into the guided mode with a specific propagation direction and specific circular polarization is

$$W_{guid} = 2\gamma_{guid} = \\ = \frac{\omega_{eg} \tilde{\beta}' \langle \alpha_e F_e M_e | d_\sigma | \alpha_g F_g M_g \rangle^2}{2\varepsilon_0 \hbar} \left|\tilde{\boldsymbol{\mathcal{E}}}\right|^2, \tag{16}$$

where $\langle \alpha_e F_e M_e | d_\sigma | \alpha_g F_g M_g \rangle$ is the projection of the atomic dipole moment on the field direction [4], $\sigma = \pm 1$, and $\omega_{eg} = \omega_{\alpha_e F_e; \alpha_g F_g}$. The last equation can be rewritten in a convenient form by introducing the dimensionless derivative $\beta' = d\beta/dk = c\tilde{\beta}'$ and using an expression for the dipole matrix element through the $3j$-symbols,

$$\langle \alpha_e F_e M_e | d_\sigma | \alpha_g F_g M_g \rangle = \\ = (-1)^{F_e - M_e} \begin{pmatrix} F_e & 1 & F_g \\ -M_e & \sigma & M_g \end{pmatrix} \times \\ \times \langle \alpha_e F_e || d || \alpha_g F_g \rangle, \tag{17}$$

and an equation for the spontaneous decay rate from the excited state $|\alpha_e F_e\rangle$ to the ground state $|\alpha_g F_g\rangle$:

$$W_{sp} = 2\gamma_{sp} = \frac{1}{4\pi\varepsilon_0} \frac{4 \left|\langle \alpha_e F_e \| d \| \alpha_g F_g \rangle\right|^2 \omega_{eg}^3}{3(2F_e + 1)\hbar c^3}. \tag{18}$$

This gives

$$W_{guid} = 2\gamma_{guid} = W_{sp} \frac{3\lambda^2 \beta'}{8\pi} (2F_e + 1) \times \\ \times \begin{pmatrix} F_e & 1 & F_g \\ -M_e & \sigma & M_g \end{pmatrix}^2 |\tilde{\boldsymbol{\mathcal{E}}}|^2. \tag{19}$$

We note that the reduced dipole matrix element for the hyperfine structure transition is expressed through the reduced dipole matrix element $\langle \alpha_e \| d \| \alpha_g \rangle$ for the fine structure transition as

$$\langle \alpha_e F_e \| d \| \alpha_g F_g \rangle = \\ = (-1)^{J_e + I + F_g + 1} \sqrt{(2F_g + 1)(2F_e + 1)} \times \\ \times \begin{Bmatrix} J_e & F_e & I \\ F_g & J & 1 \end{Bmatrix} \langle \alpha_e \| d \| \alpha_g \rangle. \tag{20}$$

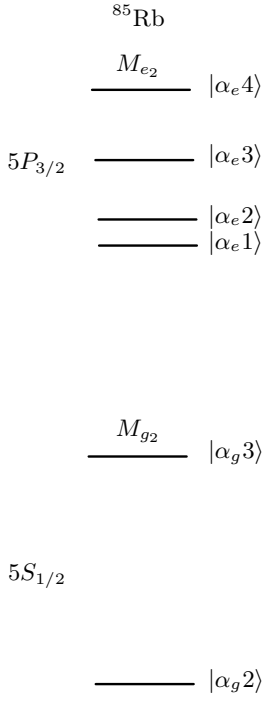

Fig. 3. The atomic level scheme describing the hyperfine structure sublevels in the excited and ground states of an ^{85}Rb atom

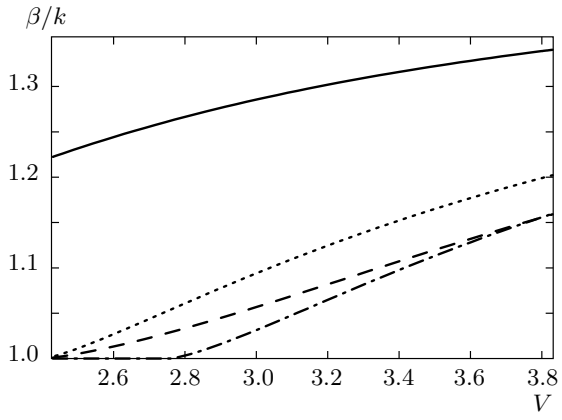

Fig. 4. Normalized propagation constant β/k as a function of the V-number for the guided modes HE_{11} (solid line), TE_{01} (dotted line), TM_{01} (dashed line), and HE_{21} (dot-dashed line)

3. DECAY RATES FOR Rb ATOMS

We estimate spontaneous emission rates into the first four guided modes for ^{85}Rb atoms (Fig. 3). We assume that the atoms emit fluorescence light into an optical nanofiber made of fused silica with the permittivity $\varepsilon_1 = n_1^2 = 2.1$. The ^{85}Rb atoms are assumed to be excited at the $5S_{1/2}$–$5P_{3/2}$ optical dipole transition, with the wavelength $\lambda = 780$ nm. The spontaneous decay rate from the upper $5P$ state into free space is $W_0 = 2\pi\cdot$ 6 MHz. We choose the fiber radius $a = 400$ nm at which, under the chosen parameters, the V-number has the value

$$V = \frac{2\pi a}{\lambda}\sqrt{n_1^2 - n_2^2} = 3.38.$$

At this value of the V-number, atomic fluorescence can excite four fiber modes, HE_{11}, TE_{01}, TM_{01}, and HE_{21}, with the respective propagation constants $\beta/k = 1.315$, 1.150, 1.105, 1.095. Eigenvalue equations for the propagation constants and electric field distributions for the chosen modes are given in Appendix. The dependence of the propagation constants β on the V-number is shown in Fig. 4 for the region

$$2.405 < V = \frac{2\pi a}{\lambda}\sqrt{n_1^2 - n_2^2} < 3.832,$$

where the fundamental mode HE_{11} coexists with the first three higher-order modes TE_{01}, TM_{01}, and EH_{21}. For a fused silica fiber located in the vacuum, with $n_1 = 1.45$ and $n_2 = 1$, the above condition defines the region of the fiber radii as $0.365\lambda < a < 0.581\lambda$.

We evaluate spontaneous decay rates of ^{85}Rb atoms into the nanofiber guided modes for different excited-state magnetic sublevels. Evaluation for each guided mode is based on the electric field distribution given in Appendix.

The spontaneous decay rate into the fundamental mode HE_{11} with a given propagation direction $+z$ or $-z$ and a given circular polarization $\sigma = +1$ for the specific initial atomic state $|F_e, M_e\rangle$ is

$$W_{guid}(r) = 2\gamma_{guid} = W_{sp}\frac{3\lambda^2\beta'}{8\pi^2 a^2}\times$$
$$\times\frac{J_1^2(ha)/K_1^2(qa)}{n_1^2N_1 + n_2^2N_2}(2F_e+1)\times$$
$$\times\begin{pmatrix} F_e & 1 & F_g \\ -M_e & \sigma & M_g \end{pmatrix}^2\left\{K_1^2(qr) + \right.$$
$$\left. + \frac{\beta^2}{2q^2}\left[(1-s)^2K_0^2(qr) + (1+s)^2K_2^2(qr)\right]\right\}. \quad (21)$$

The spontaneous decay rate into the TE_{01} mode with the specific propagation direction $+z$ or $-z$ and specific circular polarization $\sigma = +1$ for a given initial atomic state $|F_e, M_e\rangle$ is

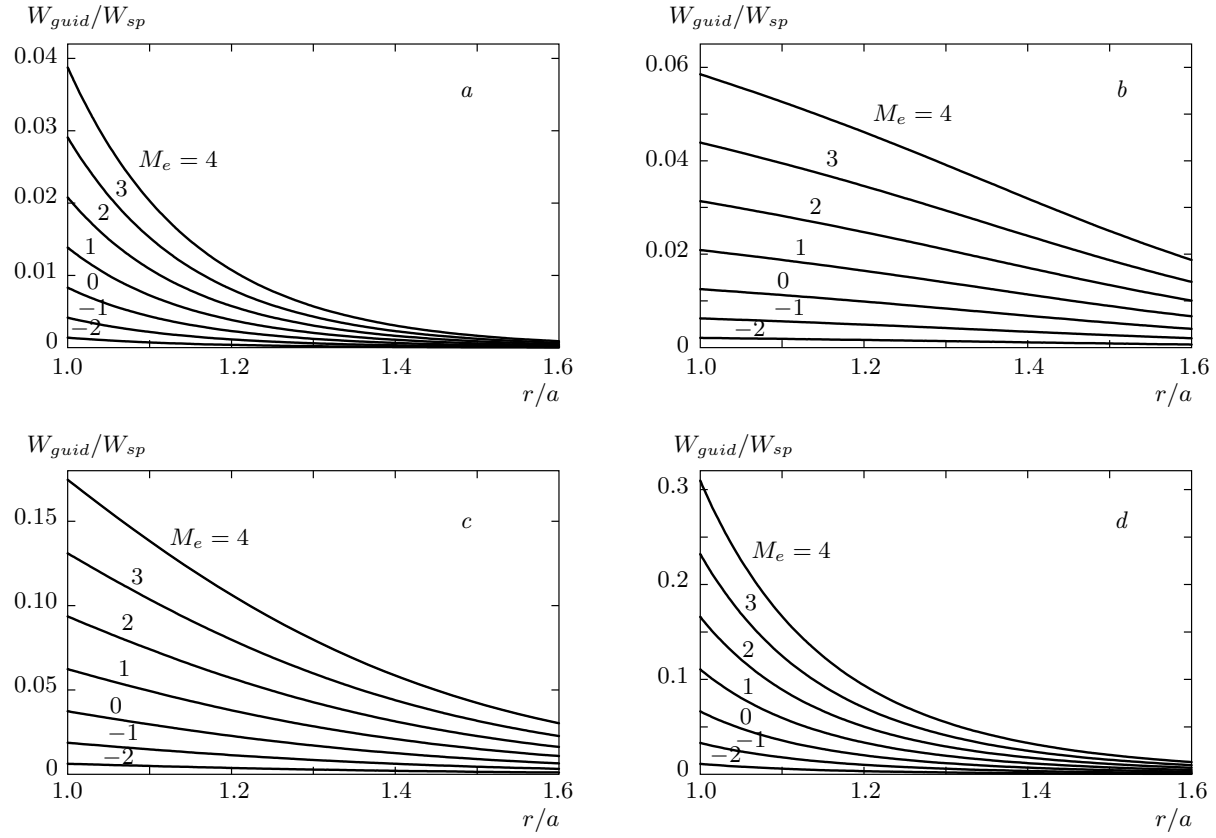

Fig. 5. Normalized pumping rates for the fundamental guided modes (a) HE_{11}, (b) TE_{01}, (c) TM_{01}, and (d) HE_{21} as functions of the distance between the ^{85}Rb atom prepared in the hyperfine structure state $F_e = 4, M_e = -2, -1, \ldots, 4$ and the axis of the optical nanofiber with the radius $a = 400$ nm

$$W_{guid}(r) = W_{sp}\frac{3\lambda^2\beta'}{8\pi^2 q^2 a^4}\frac{1}{n_1^2 P_1 + n_2^2 P_2}(2F_e+1)\times \times \begin{pmatrix} F_e & 1 & F_g \\ -M_e & \sigma & M_g \end{pmatrix}^2 K_1^2(qr). \quad (22)$$

The spontaneous decay rate into the TM_{01} mode with the specific propagation direction $+z$ or $-z$ and polarization $\sigma = +1$ considered for the specific initial atomic state $|F_e, M_e\rangle$ is

$$W_{guid}(r) = W_{sp}\frac{3\lambda^2\beta'}{8\pi^2 a^2}\frac{1}{n_1^2 Q_1 + n_2^2 Q_2}(2F_e+1)\times \times \begin{pmatrix} F_e & 1 & F_g \\ -M_e & \sigma & M_g \end{pmatrix}^2 \times \times \left(K_0^2(qr) + \frac{\beta^2}{q^2}K_1^2(qr)\right). \quad (23)$$

The spontaneous decay rate into the HE_{21} mode with the specific propagation direction $+z$ or $-z$ and polarization $\sigma = +1$ considered for the specific initial atomic state $|F_e, M_e\rangle$ is

$$W_{guid}(r) = W_{sp}\frac{3\lambda^2\beta'}{8\pi^2 a^2}\frac{J_2^2(ha)/K_2^2(qa)}{n_1^2 R_1 + n_2^2 R_2}(2F_e+1)\times \times \begin{pmatrix} F_e & 1 & F_g \\ -M_e & \sigma & M_g \end{pmatrix}^2 \left\{K_2^2(qr) + + \frac{\beta^2}{2q^2}\left[(1-u)^2 K_1^2(qr) + (1+u)^2 K_3^2(qr)\right]\right\}. \quad (24)$$

We choose the practically important case of a cyclic dipole transition $F_e = 4 - F_g = 3$ and consider the $\sigma = 1$ polarized guided mode for definiteness. The normalized spontaneous decay rates $W_{guid}/W_{sp} = \gamma_{guid}/\gamma_{sp}$ for the initial atomic states $F_e = 4$, $M_e = -2, -3, \ldots, 4$ are shown in Fig. 5 as functions of the distance between the atom and the optical nanofiber axis.

As another example, we compare spontaneous emission rates into the fundamental guiding mode for two different hyperfine structure transitions $F_e = 3$, $M_e = 3 \to F_g = 3$, $M_g = 3$ and $F_e = 3$, $M_e = 3 \to F_g = 2$, $M_g = 2$. The position dependence of the spontaneous decay rates for these transitions is shown in Fig. 6.

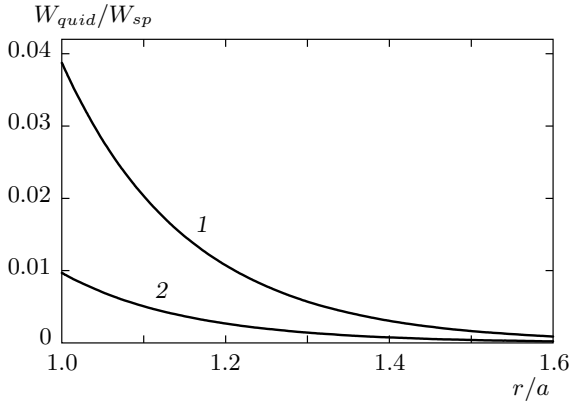

Fig. 6. Spontaneous decay rates into the fundamental guided mode HE_{11} for the hyperfine structure transitions $F_e = 3,\ M_e = 3 \to F_g = 3,\ M_g = 3$ (curve *1*) and $F_e = 3,\ M_e = 3 \to F_g = 2,\ M_g = 2$ (curve *2*)

4. CONCLUSION

We have examined the efficiency of coupling the fluorescence emitted by a multilevel atom possessing a hyperfine structure into an optical nanofiber and found that the decay rates strongly depend on the initial atomic state. Numerical evaluations for Rb atoms show that the decay rates for different magnetic sublevels can differ by an order of magnitude.

We also found that the decay rates into the higher-order modes can be about 5 to 10 times higher than that into the fundamental mode. This can be explained by the proportionality of the spontaneous decay rate to the intensity of the vacuum guided mode of a nanofiber. Because the evanescent "tail" of the higher-order modes exceeds that of the fundamental mode, the higher-order modes have a higher rate of the excitation by fluorescent light of atoms located outside the fiber.

A considerable increase in the spontaneous decay rate for higher-order modes can be important in the experiments on excitation of optical nanofibers by the fluorescent emission of atom clouds confined around the nanofiber. The high pumping rate of higher-order modes in optical nanofibers may find important applications in quantum optics and metrology, including the creation of new trapping geometries for atoms, new types of coupling to microresonators, new schemes for evanescent field sensing of atoms, and high-accuracy position detection of atoms around nanofibers.

This work was supported by the RFBR (Grant No. 12-02-00867-a).

APPENDIX

Propagation constants and electric fields of the four lowest guided modes

For the fundamental guided mode HE_{11}, the propagation constant is defined by the eigenvalue equation

$$\frac{J_0(ha)}{haJ_1(ha)} = -\frac{n_1^2+n_2^2}{2n_1^2}\frac{K_1'(qa)}{qaK_1(qa)} + \frac{1}{h^2a^2} - \frac{n_1^2-n_2^2}{n_1^2}\times \\ \times\left[\left(\frac{K_1'(qa)}{2qaK_1(qa)}\right)^2 + \left(\frac{n_1k\beta}{a^2h^2q^2}\right)^2\right]^{1/2}. \quad (A.1)$$

For the TE_{01} mode, the propagation constant is defined by the eigenvalue equation

$$\frac{J_1(ha)}{haJ_0(ha)} = -\frac{K_1(qa)}{qaK_0(qa)}, \quad (A.2)$$

for the TM_{01} mode, by the eigenvalue equation

$$\frac{J_1(ha)}{haJ_0(ha)} = -\frac{n_2^2}{n_1^2}\frac{K_1(qa)}{qaK_0(qa)}, \quad (A.3)$$

and for the mode HE_{21}, by the eigenvalue equation

$$\frac{J_1(ha)}{haJ_2(ha)} = -\frac{n_1^2+n_2^2}{2n_1^2}\frac{K_2'(qa)}{qaK_2(qa)} + \frac{2}{h^2a^2} - \frac{n_1^2-n_2^2}{n_1^2}\times \\ \times\left[\left(\frac{K_2'(qa)}{2qaK_2(qa)}\right)^2 + \left(\frac{2n_1k\beta}{a^2h^2q^2}\right)^2\right]^{1/2}, \quad (A.4)$$

where J_m are Bessel functions of the first kind, K_m are modified Bessel functions of the second kind, $k = \omega/c$, a is the fiber radius, and

$$h = \sqrt{n_1^2k^2 - \beta^2}, \quad q = \sqrt{\beta^2 - n_2^2k^2}.$$

The spatial distribution of the electric field for any guided mode can be written using the cylindrical unit vectors $\mathbf{e}_r$, $\mathbf{e}_\varphi$, and $\mathbf{e}_z$:

$$\tilde{\boldsymbol{\mathcal{E}}} = \mathbf{e}_r\tilde{\mathcal{E}}_r + \mathbf{e}_\varphi\tilde{\mathcal{E}}_\varphi + \mathbf{e}_z\tilde{\mathcal{E}}_z.$$

For the chosen four lowest guided modes, the cylindrical components of a normalized electric field amplitude are given by the following equations. The cylindrical components of a normalized electric field amplitude for the HE_{11} mode in the core region are [20]

$$\tilde{\mathcal{E}}_r = iA\frac{q}{h}\frac{K_1(qa)}{J_1(ha)}\left[(1-s)J_0(hr) - \right. \\ \left. - (1+s)J_2(hr)\right], \\ \tilde{\mathcal{E}}_\varphi = -A\frac{q}{h}\frac{K_1(qa)}{J_1(ha)}\left[(1-s)J_0(hr) + \right. \quad (A.5) \\ \left. + (1+s)J_2(hr)\right], \\ \tilde{\mathcal{E}}_z = 2A\frac{q}{\beta}\frac{K_1(qa)}{J_1(ha)}J_1(hr),$$

and those outside the core region are

$$\begin{aligned}\tilde{\mathcal{E}}_r &= iA\left[(1-s)K_0(qr)+(1+s)K_2(qr)\right],\\ \tilde{\mathcal{E}}_\varphi &= -A\left[(1-s)K_0(qr)-(1+s)K_2(qr)\right],\\ \tilde{\mathcal{E}}_z &= 2A\,(q/\beta)\,K_1(qr).\end{aligned} \tag{A.6}$$

In the above equations, s is a dimensionless parameter such that

$$s=\frac{1/h^2a^2+1/q^2a^2}{S},$$

where the denominator is

$$S=J_1'(ha)/haJ_1(ha)+K_1'(qa)/qaK_1(qa).$$

The normalization constant defined from Eq. (12) is

$$A=\frac{\beta}{2q}\,\frac{J_1\,(ha)\,/K_1\,(qa)}{\sqrt{2\pi a^2\,(n_1^2N_1+n_2^2N_2)}},$$

where

$$\begin{aligned}N_1=\frac{\beta^2}{4h^2}\left\{(1-s)^2\left[J_0^2(ha)+J_1^2(ha)\right]+\right.\\ \left.+\,(1+s)^2\left[J_2^2(ha)-J_1(ha)J_3(ha)\right]\right\}+\\ +\frac{1}{2}\left[J_1^2(ha)-J_0(ha)J_2(ha)\right]\end{aligned}$$

and

$$\begin{aligned}N_2=\frac{J_1^2(ha)}{2K_1^2(qa)}\times\\ \times\left\{\frac{\beta^2}{2q^2}\left[(1-s)^2\left[K_1^2(qa)-K_0^2(qa)\right]-\right.\right.\\ -\,(1+s)^2\left[K_2^2(qa)-K_1(qa)K_3(qa)\right]\Big]-\\ \left.-\,K_1^2(qa)+K_0(qa)K_2(qa)\right\}.\end{aligned}$$

For the TE_{01} mode in the core region,

$$\begin{aligned}\tilde{\mathcal{E}}_r &= 0,\\ \tilde{\mathcal{E}}_\varphi &= \frac{i}{\sqrt{\pi}ha^2}\,\frac{K_0(qa)/J_0(ha)}{\sqrt{n_1^2P_1+n_2^2P_2}}J_1(hr),\\ \tilde{\mathcal{E}}_z &= 0,\end{aligned} \tag{A.7}$$

and outside the core region,

$$\begin{aligned}\tilde{\mathcal{E}}_r &= 0,\\ \tilde{\mathcal{E}}_\varphi &= -\frac{i}{\sqrt{\pi}qa^2}\,\frac{1}{\sqrt{n_1^2P_1+n_2^2P_2}}K_1(qr),\\ \tilde{\mathcal{E}}_z &= 0,\end{aligned} \tag{A.8}$$

where

$$\begin{aligned}P_1=\frac{1}{a^2h^2}\,\frac{K_0^2(qa)}{J_0^2(ha)}\left[J_1^2(ha)-J_0(ha)J_2(ha)\right],\\ P_2=\frac{1}{a^2q^2}\left[K_0(qa)K_2(qa)-K_1^2(qa)\right].\end{aligned}$$

For the TM_{01} mode in the core region,

$$\begin{aligned}\tilde{\mathcal{E}}_r &= -\frac{i\beta}{\sqrt{\pi}ha}\,\frac{K_0(qa)/J_0(ha)}{\sqrt{n_1^2Q_1+n_2^2Q_2}}J_1(hr),\\ \tilde{\mathcal{E}}_\varphi &= 0,\\ \tilde{\mathcal{E}}_z &= \frac{1}{\sqrt{\pi}a}\,\frac{K_0(qa)/J_0(ha)}{\sqrt{n_1^2Q_1+n_2^2Q_2}}J_0(hr),\end{aligned} \tag{A.9}$$

and outside the core region,

$$\begin{aligned}\tilde{\mathcal{E}}_r &= \frac{i\beta}{\sqrt{\pi}qa}\sqrt{n_1^2Q_1+n_2^2Q_2}K_1(qr),\\ \tilde{\mathcal{E}}_\varphi &= 0,\\ \tilde{\mathcal{E}}_z &= \frac{1}{\sqrt{\pi}a}\sqrt{n_1^2Q_1+n_2^2Q_2}K_0(qr),\end{aligned} \tag{A.10}$$

where

$$Q_1=\frac{K_0^2(qa)}{J_0^2(ha)}\left[J_0^2(ha)+\frac{n_1^2k^2}{h^2}J_1^2(ha)-\frac{\beta^2}{h^2}J_0(ha)J_2(ha)\right],$$

$$Q_2=\frac{\beta^2}{q^2}K_0(qa)K_2(qa)-K_0^2(qa)-\frac{n_2^2k^2}{q^2}K_1^2(qa).$$

For the HE_{21} mode in the core region,

$$\begin{aligned}\tilde{\mathcal{E}}_r &= A_{21}\frac{i\beta}{2h}\left[(1-u)J_1(hr)-(1+u)J_3(hr)\right],\\ \tilde{\mathcal{E}}_\varphi &= -A_{21}\frac{\beta}{2h}\left[(1-u)J_1(hr)+(1+u)J_3(hr)\right],\\ \tilde{\mathcal{E}}_z &= A_{21}J_2(hr),\end{aligned} \tag{A.11}$$

and outside the core region,

$$\begin{aligned}\tilde{\mathcal{E}}_r &= A_{21}\frac{i\beta}{2q}\,\frac{J_2(ha)}{K_2(qa)}\times\\ &\quad\times\left[(1-u)K_1(qr)+(1+u)K_3(qr)\right],\\ \tilde{\mathcal{E}}_\varphi &= -A_{21}\frac{\beta}{2q}\,\frac{J_2(ha)}{K_2(qa)}\times\\ &\quad\times\left[(1-u)K_1(qr)-(1+u)K_3(qr)\right],\\ \tilde{\mathcal{E}}_z &= A_{21}\frac{J_2(ha)}{K_2(qa)}K_2(qr).\end{aligned} \tag{A.12}$$

In the above equations, u is a dimensionless parameter such that

$$u=\frac{2(1/h^2a^2+1/q^2a^2)}{J_2'(ha)/haJ_2(ha)+K_2'(qa)/qaK_2(qa)}.$$

The normalization constant defined from Eq. (12) is

$$A_{21} = \frac{1}{\sqrt{\pi}a\sqrt{n_1^2 R_1 + n_2^2 R_2}},$$

where

$$R_1 = J_2^2(ha) - J_1(ha)J_3(ha) + \\ + \frac{\beta^2}{2h^2}\left[(1-u)^2\left(J_1^2(ha) - J_0(ha)J_2(ha)\right) + \right. \\ \left. + (1+u)^2\left(J_3^2(ha) - J_2(ha)J_4(ha)\right)\right],$$

$$R_2 = \frac{J_2^2(ha)}{K_2^2(qa)}\left\{K_1(qa)K_3(qa) - K_2^2(qa) + \right. \\ + \frac{\beta^2}{2q^2}\left[(1-u)^2\left(K_0(qa)K_2(qa) - K_1^2(qa)\right) + \right. \\ \left.\left. + (1+u)^2\left(K_2(qa)K_4(qa) - K_3^2(qa)\right)\right]\right\}.$$

REFERENCES

1. H. Nha and W. Jhe, Phys. Rev. A **56**, 2213 (1997).
2. T. Søndergaard and B. Tromborg, Phys. Rev. A **64**, 033812 (2001).
3. V. V. Klimov and M. Ducloy, Phys. Rev. A **69**, 013812 (2004).
4. F. Le Kien, S. Dutta Gupta, V. I. Balykin, and K. Hakuta, Phys. Rev. A **72**, 032509 (2005).
5. G. Sague, E. Vetsch, W. Alt et al., Phys. Rev. Lett. **99**, 163602 (2007).
6. K. P. Nayak, P. N. Melentiev, M. Morinaga et al., Opt. Express **15**, 5431 (2007).
7. L. Russell, D. A. Gleeson, V. G. Minogin, and S. N. Chormaic, J. Phys. B **42**, 185006 (2009).
8. A. Afanasiev and V. Minogin, Phys. Rev. A **82**, 052903 (2010).
9. R. Schmidt, S. N. Chormaic, and V. G. Minogin, J. Phys. B **44**, 015004 (2011).
10. M. Frawley, V. G. Minogin, and S. N. Chormaic, Phys. Scripta **85**, 058103 (2012).
11. J. P. Dowling and J. Gea-Banacloche, Adv. At. Mol. Opt. Phys. **36**, 1 (1996).
12. V. I. Balykin, K. Hakuta, F. Le Kien et al., Phys. Rev. A **70**, 011401(R) (2004).
13. G. Sagué, A. Baade, and A. Rauschenbeutel, New J. Phys. **10**, 113008 (2008).
14. E. Vetsch, D. Reitz, G. Sagu et al., Phys. Rev. Lett. **104**, 203603 (2010).
15. F. Le Kien, S. D. Gupta, K. P. Nayak, and K. Hakuta, Phys. Rev. A **72**, 063815 (2005).
16. S. Mancini and S. Bose, Phys. Rev. A **70**, 022307 (2004).
17. A. V. Masalov and V. G. Minogin, Laser Phys. Lett. **10**, 075203 (2013).
18. I. I. Sobelman, *Atomic Spectra and Radiative Transitions*, Springer-Verlag, Berlin (1979).
19. R. Loudon, *The Quantum Theory of Light*, Clarendon, Oxford (1973).
20. A. W. Snyder and J. D. Love, *Optical Waveguide Theory*, Chapman and Hall, New York (1983).